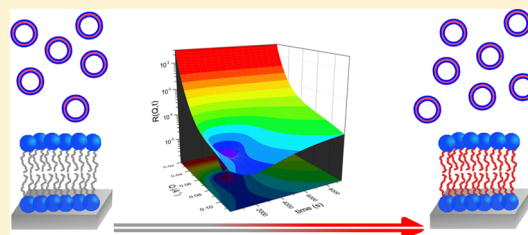


Lipid Exchange and Flip-Flop in Solid Supported Bilayers

Yuri Gerelli,^{*,†} Lionel Porcar,[†] Lucia Lombardi,^{‡,†} and Giovanna Fragneto[†][†]Institut Laue-Langevin, 6, rue Jules Horowitz, 38042, Grenoble CEDEX 9, France[‡]Department of Chemistry, University of Naples Federico II, Corso Umberto I, 40, 80138 Naples, Italy

Supporting Information

ABSTRACT: Inter- and intrabilayer transfer of phospholipid molecules was investigated by neutron reflectometry. The structure of solid supported lipid bilayers exposed to a solution of isotopically labeled vesicles was monitored as a function of temperature, time, and vesicle concentration. Lipid interbilayer exchange was shown to be the time limiting process, while lipid intrabilayer movement, the so-called flip-flop, was too fast to be visualized within the experimental acquisition time. The exchange process was characterized by an Arrhenius-like behavior and the activation energy of the process was concentration-independent. The results are discussed and compared extensively with the literature available on the topic.



INTRODUCTION

Lipid translocation in membranes is a crucial process in biological sciences which is still far from being understood and characterized. In nature, the lipid distribution across the inner and outer leaflet of cell membranes is asymmetric,^{1,2} and this asymmetry plays a prominent role during cell fusion, activation of the coagulation processes, and recognition and removal of apoptotic cell corpses by macrophages.³ It is hypothesized that lipid asymmetry in natural membranes is promoted by the action of specific enzymes and by retentive mechanisms that trap lipids in one leaflet of the bilayer.⁴ In the absence of these enzymes, any induced asymmetry can be spontaneously lost. Both promotion and loss of asymmetry result from trans-membrane migration of lipid molecules, a process commonly called lipid *flip-flop*. Another process that involves migration of lipid molecules in cells is the exchange of lipid molecules between two different membranes. This process is commonly called *lipid exchange*. These two processes do not have the same biological function and origin, but they have in common the extraction/insertion of an individual lipid molecule from/to a bilayer leaflet. Because of this, many studies investigating lipid flip-flop also dealt with lipid exchange and vice versa.

From a biophysical point-of-view, studies of the characteristics of these processes in model systems have been conducted since the late 1960s.^{5–16} None of them is conclusive and several discrepancies exist in the lipid flip-flop mechanism and involved time scales. Lipid exchange was studied in combination with lipid flip-flop in many of the cited works, and one of the most widely studied systems is bilayer 1,2-dimyristoyl-*sn*-glycero-3-phosphocholine (DMPC).^{11,14,17} One attempt to directly visualize lipid flip-flop was made by John and co-workers¹² by using fluorescent phospholipid markers in DMPC vesicles. They measured a rate increase in the trans-bilayer movement of the dyes going through the melting phase transition of the DMPC molecules. The typical dye flip-flop kinetics took place on the 1–2 min time scale. Older studies made use of modified

lipid molecules or the inclusion of fluorescent probes or dyes in lipid membranes. The lipid exchange process was investigated by measuring the total fluorescence of a solution obtained by mixing fluorescent and nonfluorescent vesicle samples. The same method was widely used to study the migration of dyes like fluorescent cholesterol molecules. However, since lipid trans-membrane movement takes place inside an individual vesicle, it was difficult to visualize lipid migration directly due to the lack of spatial resolution in many of the techniques employed. Nowadays, it is well-known that these molecular modifications could have an impact on the overall macroscopic dynamics of the molecules constituting the lipid matrix.¹⁸ For this reason newer approaches, based on the use of advanced experimental techniques exploiting the isotopic substitution effect, were developed in order to get better understanding of these processes. This is the case of small angle neutron scattering (SANS)¹⁴ and sum-frequency vibrational spectroscopy (SFVS).^{13,15,16} In this respect, the perturbation induced in the sample by using isotopically substituted molecules was considered almost negligible for the determination of structural and dynamical features.^{19,20} A recent study by our group probed the loss of asymmetry in a solid supported lipid bilayer across its main phase transition by using neutron reflectometry (NR).²¹ This technique is one of the most suitable techniques for the investigation of the absolute composition and the relative location of molecules within a bilayer and at its interfaces.²² The great difference of the neutron–nuclei interaction upon isotopic exchange makes NR particularly sensitive to detect displacement of material along the normal direction of a bilayer.²³ As shown elsewhere²¹ if any compositional asymmetry involving segregation of deuterated and hydrogenated molecules is present in a lipid bilayer, the

Received: July 16, 2013

Revised: September 5, 2013

Published: September 17, 2013

recorded reflectivity contains a clear signature of the asymmetric structure. We showed that the starting asymmetry of an adsorbed DMPC:DSPC bilayer was lost once the overall bilayer entered the liquid phase. It was impossible to measure any intermediate state of the transition taking place in less than 1 min.²¹

The measurements were performed going through the lipid melting phase transition, i.e., going from the gel, L_{β} , to the fluid, L_{α} phase. It could be argued that the melting transition could release enough energy in the sample to make the flip-flop movement faster. Attempts to measure lipid flip-flop without the use of additional guest molecules and without crossing the sample melting phase transition were done by exploiting the already mentioned SFVS; Conboy and co-workers^{13,15,16} found that the characteristic rate of trans-bilayer process in DMPC increased as the temperature was increased. It was not possible to measure the rate near or above the gel-to-liquid phase-transition temperature due to the rapid movement of lipids at these temperatures. The sample was prepared by Langmuir–Blodgett/Langmuir–Schaefer (LB/LS) techniques, depositing DMPC molecules in one leaflet and d54-DMPC (chain deuterated lipids) in the opposite leaflet. It has been shown²¹ that LB/LS techniques cannot be used to prepare asymmetric solid supported bilayers in the liquid phase. In fact, mixing of the materials occurs during the application of LS stage. This aspect did not allow flip-flop rearrangement in bilayers as prepared in the L_{α} phase to be studied in either of the NR and SFVS experiments.^{13,21} Nevertheless, SFVS indicated that, even in the gel phase, the process becomes faster as the temperature increases, suggesting a quicker flip-flop in the biologically relevant liquid phase.

An “in solution” approach based on the use of isotopically labeled molecules was developed independently by Nakano and co-workers¹⁴ and Garg and co-workers²⁴ to investigate the exchange and the flip-flop of DMPC and cholesterol molecules, respectively. In the case of DMPC they measured the time dependence of the integrated SANS intensity during the mixing of DMPC and d54-DMPC vesicles in a 1:1 ratio.¹⁴ Inter- and intravesicle lipid rearrangement gave rise to a final homogeneous sample composed of identical vesicles, each of them containing 1:1 DMPC:d54-DMPC molecules. The integrated SANS intensity time dependence was analyzed in terms of a 2-step process with lipid exchange and flip-flop occurring on different and detectable time-scales. It is worth noting that lipid flip-flop appeared to be a much slower process from the analysis of the SANS data than that derived from SFVS experiments.

It is widely accepted that exchange and flip-flop are thermally activated processes. A summary of values for the activation energies for lipid exchange (E_a^{ex}) and lipid flip-flop (E_a^f) taken from the above listed experiments are given in Table 1. Experiments performed crossing a phase transition are not reported in the table. From the values it is clear that several discrepancies are still to be solved regarding both processes.

In the present work we combine NR measurements with the “in solution” approach already used in SANS.^{14,24} We follow the lipid exchange between an adsorbed bilayer exposed to a vesicle solution made with the same lipid molecules but with different isotopic composition. It was possible to determine the temperature and concentration dependence of the exchange process as well as the intermediate relative composition of the adsorbed bilayer. While the resulting activation energy due to lipid exchange was in perfect agreement with that reported in

Table 1. Experimental Conditions and the Activation Energies for Lipid Exchange (E_a^{ex}) and for Lipid Flip-Flop (E_a^f) Published for DMPC Based Systems^a

sample	state	E_a^{ex} (KJ/mol)	E_a^f (KJ/mol)
LUV-DMPC ¹⁴	100 nm size, above T_m	85 ± 2	64 ± 2
PSLB-DMPC ^{13,16}	LB/LS, below T_m	n.a.	230 ± 10
	LB/LS, above T_m	n.a.	~0 ^b
SPIN-DMPC ^{11,17}	LUV 100 nm size, above T_m	105 ± 4	<105
	SUV 23 nm size, above T_m	84 ± 17	≥84

^aAbbreviations: SUV = small uni-lamellar vesicles, LUV = large uni-lamellar vesicles, SPIN = radio-labeled DMPC, LB/LS = Langmuir–Blodgett–Langmuir–Schaefer deposition technique. ^bToo low to be measured.

ref 14, the activation energy for lipid flip-flop turned out to be too low to measure. In fact the time-dependence of the reflectivity curves, as described in analogy to the SANS integrated intensity, showed a single exponential behavior showing lipid exchange to be the only time-limiting process.

MATERIALS AND METHODS

Solid supports for neutron reflectometry were 8 × 5 × 1 cm³ silicon single crystals cut and polished along the (111) plane. They were cleaned for 15 min in a mild-piranha solution (1:4:5 H₂O₂:H₂SO₄:H₂O) at 85 °C and subsequently exposed to O₃ atmosphere by UV-ozone apparatus rendering the surface more hydrophilic. 1,2-Dimyristoyl-*sn*-glycero-3-phosphocholine (DMPC) and 1,2-dimyristoyl(d54)-*sn*-glycero-3-phosphocholine (d54-DMPC) were purchased from Avanti Polar Lipids (Alabaster, AL). Unilamellar DMPC and d54-DMPC vesicle solutions were prepared in high purity D₂O (Sigma-Aldrich Inc., USA) by the extrusion method²⁵ through a polycarbonate membrane with pores of 100 nm nominal size.

Standard Reflectometry Measurements. Specular reflectivity, $R(Q)$, defined as the ratio between the reflected and the incident intensities of a neutron beam, is measured as a function of the wave vector transfer, Q , perpendicular to the reflecting surface. Neutron reflectometry experiments were performed on the silicon/water interface using the reflectometers FIGARO²⁶ and D17²⁷ (Institut Laue-Langevin, Grenoble, France) and INTER²⁸ (ISIS facility, Rutherford Appleton Laboratory, Chilton, UK). Time-of-flight measurements were performed using different angular orientations for each instrument resulting in a covered Q -range from 0.005 to 0.3 Å⁻¹.

Solid supported bilayers were deposited by vesicle fusion method^{29,30} using vesicles in pure water at 0.5 mg/mL injected directly into the laminar flow cells provided at the instruments. These cells could also be flushed with water (D₂O, H₂O, or a mixture) to remove the remaining vesicles after the bilayer formation and to apply the well-known contrast variation method.³¹ For this purpose high purity D₂O and Milli-Q water were used with the following ratios 1:0, 0.66:0.34, and 0:1, resulting in media with neutron scattering length density (SLD or ρ in the following) of 6.35, 4.00, and -0.56 (×10⁻⁶ Å⁻²), respectively. The structure of the starting deposited bilayers and of the final states reached at the end of the kinetics measurements were characterized by NR using each of the three different water solutions.

Kinetics Reflectometry Measurements. Time-dependent measurements were obtained by exposing the adsorbed

bilayer to a medium containing vesicles made of isotopically labeled DMPC molecules. H-to-D replacement kinetics were followed by exposing a starting protonated DMPC adsorbed bilayer to a 1 mg/mL d54-DMPC deuterated vesicle solution while the D-to-H ones were performed exposing a deuterated bilayer to a hydrogenated vesicle solution. This approach merges some ideas taken from SANS^{14,24} and SFVS^{13,15,16} experiments and tries to overcome some of the weak points of these techniques. For example, SFVS experiments to measure the spontaneous rearrangement of lipid molecules by flip-flop mechanism were not used to get information about lipid exchange. These measurements were conducted only at temperatures below the phase transition of the lipid species involved, i.e., in the L_β gel phase. On the other hand SANS measurements were suitable to extract precise information about the lipid exchange in L_α liquid phase. The influence of flip-flop on the bilayer structure in these measurements could not be directly determined by fitting the scattering intensity according to an asymmetric bilayer form factor. However, the analysis of the time-evolution of the SANS integrated intensity showed the need to model the overall mixing as a 2-step process, one of them being lipid exchange between different vesicles and the other the trans-membrane movement of lipid molecules inside a single vesicle.

Kinetics measurements were performed at one fixed angular configuration per instrument giving access to a Q range from 0.03 to 0.3 \AA^{-1} on INTER and from 0.015 to 0.11 \AA^{-1} on FIGARO and D17. Time-resolved reflectivity series from the supported bilayer exposed to a vesicle solution were acquired until the typical curve of a completely exchanged bilayer was obtained. The acquisition time for a single run was adjusted according to the time-dependence of the kinetics, i.e., short times at the beginning (2.5 min) and longer times toward the end of the process (10 min). To investigate the temperature dependence of the overall process, kinetics measurements were recorded at three temperatures (48, 57, and 68 °C, i.e., always with bilayer and vesicles in the fluid phase¹⁹). The concentration dependence of the overall process was investigated at two different temperatures by increasing the vesicle solution concentration up to $c = 5$ mg/mL. By using the proposed NR approach it is then possible to access information on lipid exchange in the fluid phase and to measure, if present, the structural asymmetry induced by a slower flip-flop process. A pictorial view of the possible pathways for the processes are given in Figure 1. The number of the molecules on the surface is fixed (assuming full coverage) but the vesicle concentration in the bulk can be varied easily. For instance, a concentration of 1 mg/mL of lipid in the bulk solution is 5 orders of magnitude higher than the concentration of adsorbed lipid molecules. It is important to note here that the SANS experiments were always performed with an equal concentration of hydrogenated and deuterated vesicles.

Data Analysis. The membrane scattering length density profile could be described in terms of a five-layer model for asymmetric bilayers. The symmetric ones required only four layers with the hydrocarbon core region being described as uniform among inner and outer leaflets. Details about the chosen model to describe phospholipid bilayers are given elsewhere.²¹ The 5-layer model can be summarized as being composed of (from the top silicon substrate)

1. silicon oxide (t_{ox} , f_{ox} and σ_{ox})
2. inner headgroup layer (t_{PC} , f_{PC} and σ_{PCHC})

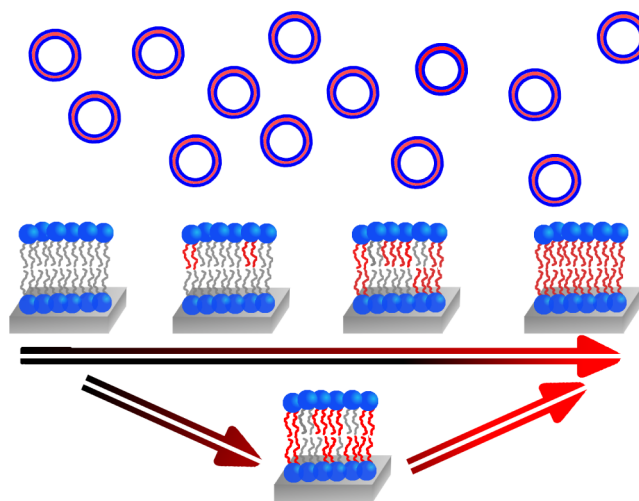


Figure 1. Pictorial view of two possible pathways of the measured kinetics. In the upper part, starting, final, and intermediate asymmetric states of the adsorbed bilayer are depicted for a slow and detectable flip-flop process. In the lower part, the symmetric structure for a non-detectable flip-flop process is given.

3. inner hydrophobic region (t_{HC} , f_{HC} and $\sigma_{HC,HC}$)
4. outer hydrophobic region (t_{HC} , f_{HC} and $\sigma_{HC,PC}$)
5. outer headgroup layer (t_{PC} , f_{PC} and σ_{PCW})

In the case of symmetric bilayers, the third and fourth layers were replaced by a unique layer characterized by thickness t_{HC} , water content f_{HC} , and roughness σ_{HCPC} .

Several physical constraints were applied to reduce the number of free parameters during the fitting procedure. Since only the hydrophobic portion of the lipid molecules was isotopically substituted the inner and outer headgroup layers could be described by the same set of structural parameters, with the exception of the roughness that in one case was between inner headgroup and hydrophobic core (σ_{PCHC}) and in the other case was between the outer layer and the medium (σ_{PCW}).

The SLD of the i -th layer was not a free parameter and was defined as

$$\rho_i = f_i \rho_s + (1 - f_i) \rho_i^{\text{dry}} \quad (1)$$

where ρ_s and f_i are, respectively, the SLD of the medium and its volume fraction within the i -th layer. The SLD of the dry components used were fixed to $\rho_{PC}^{\text{dry}} = 1.88 \times 10^{-6} \text{\AA}^{-2}$, $\rho_{HC}^{\text{dry}} = -0.28 \times 10^{-6} \text{\AA}^{-2}$, and $\rho_{d54-HC}^{\text{dry}} = 6.5 \times 10^{-6} \text{\AA}^{-2}$ for headgroups and hydrogenated and deuterated tails, respectively.^{32,33} During the analysis of the kinetics measurements the above structural parameters were kept fixed to values derived from the measurements reported in Figure 2. The only variable parameter was the SLD of the hydrocarbon core that was modeled by introducing the content of original material $\alpha(t)$ as

$$\rho_{HC}(t) = \begin{cases} \alpha(t) \rho_{HC} + [1 - \alpha(t)] \rho_{d54-HC} & \text{for D-to-H kinetics} \\ \alpha(t) \rho_{d54-HC} + [1 - \alpha(t)] \rho_{HC} & \text{for H-to-D kinetics} \end{cases} \quad (2)$$

where ρ_{d54-HC} and ρ_{HC} were evaluated according to eq 1. D-to-H and H-to-D kinetics were described by eq 2a and eq 2b respectively.

Data were analyzed using Aurore, a homemade software written in Matlab language³⁴ and based on the use of Minuit minimization routine.³⁵ Reflectivity curves were computed

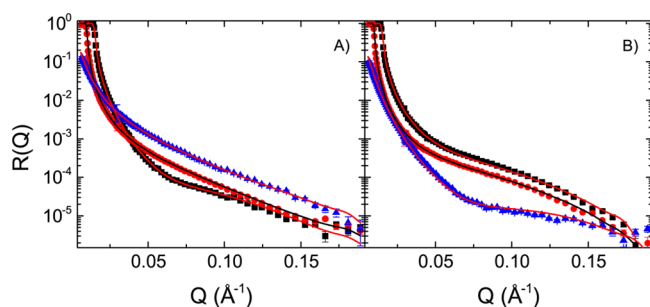


Figure 2. Experimental reflectivity curves for a d54-DMPC (A) and DMPC (B) supported bilayer in three different contrasts: D₂O (black squares), 4MW (red circles), and H₂O (blue triangles). The continuous lines are the fits obtained with the parameters listed in Table 2. Data from Figaro.

based on the Parratt formalism.³⁶ The combined use of a global fitting procedure and of the contrast variation method allowed structural details down to the Ångström length scale to be resolved.

RESULTS AND DISCUSSION

It is known that the vesicle fusion method gives rise to almost defect-free supported DMPC fluid bilayers³⁷ and therefore we preferred using this to the Langmuir–Blodgett–Langmuir–Schaefer deposition technique that could lead to a nonoptimal coverage of the substrate.³⁸ The presence of defects had to be minimized because they could affect the flip-flop kinetics, even in the gel state,¹⁶ as well as exchange. To ensure the reproducibility and the comparability of the measurements on different samples the structure of the initial bilayers was constrained to be identical within the experimental accuracy. The initial adsorbed DMPC and d54-DMPC bilayers could be modeled assuming 100% ($\pm 2\%$) coverage and using the structural parameters listed in Table 2. It may be noted that these parameters are in perfect agreement with those already published and validated for DMPC bilayers in the liquid phase found with complementary techniques providing higher spatial resolution.³³ Typical fits and resulting scattering length density profiles are given in Figures 2 and 3, while the parameters

Table 2. Parameters Obtained from the Global Fit of the Reflectivity Curves for DMPC and d54-DMPC^a

parameter	value
t_{PC}	$9 \pm 1 \text{ \AA}$
SLD_{PC}	$1.88 \times 10^{-6} \text{ \AA}^{-2}$
f_{PC}^b	0.45 ± 0.05
σ_{PCHC}	$2.0 \pm 0.5 \text{ \AA}$
t_{HC}	$27 \pm 1 \text{ \AA}$
$SLD_{d54-HC} (\times 10^{-6})$	6.5 \AA^{-2}
$SLD_{HC} (\times 10^{-6})$	-0.28 \AA^{-2}
f_{HC}^c	0.00 ± 0.02
σ_{HCPC}	$2.0 \pm 0.5 \text{ \AA}$
σ_{PCW}	$2.0 \pm 0.5 \text{ \AA}$

^aAbsolute errors were extracted from the covariance matrix³⁵ and they represent 1 standard deviation confidence interval. ^b f_{PC} indicates the volume fraction of water in the headgroup region. For the given value of $f_{PC} \sim 0.45$ the corresponding number of water molecules per lipid molecule was $n_w = 8 \pm 1$. ^c f_{HC} indicates the volume fraction of water inside the hydrocarbon region, i.e., it is related to the percentage of coverage of the substrate evaluated as $[(1 - f_{HC}) \times 100] = 100 \pm 2\%$.

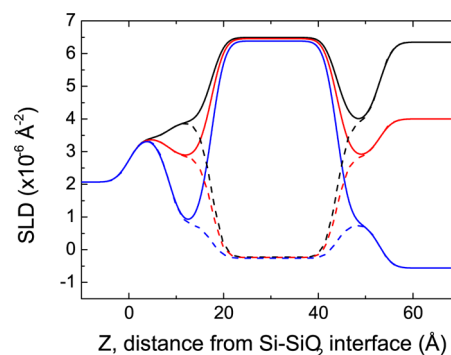


Figure 3. SLD profiles obtained from the fit of the NR data for DMPC (dashed lines) and d54-DMPC (solid lines) bilayers in three different contrasts: D₂O (black), 4MW (red) and H₂O (blue). $z = 0$ is located at the silicon/silicon-oxide interface.

obtained from the fits are listed in Table 2. The null volume fraction f_{HC} of solvent in the hydrocarbon core indicates that the bilayer is defect-free with a degree of coverage equal to $100\% \pm 2\%$ (as indicated by $(1 - f_{HC}) \times 100$ in Table 2). The structure of single component bilayers, at the length-scales probed by NR, was expected to be symmetric with respect to the middle-point of the bilayer allowing the use of the 4-layer model as previously described.

Traces of Asymmetry. If the lipid flip-flop depicted in Figure 1 takes place on a longer time scale than the lipid exchange, then it would be perfectly detectable during NR kinetics measurements. It would still be detectable even if the process was faster than the exchange but slower than the typical acquisition time used in the experiment. Traces of asymmetry were sought by using the 5-layer model described in the data analysis section. Because the isotopic substitution does not affect the structure of DMPC molecules (molecular volumes differ by less than 1%³²), thicknesses and water fractions were constrained to the same value, i.e., $t_{HC_i} = t_{HC_o}$ and $f_{HC_i} = f_{HC_o}$. The only independent parameters were therefore the SLD values, $\rho_{HC_i}(t)$ and $\rho_{HC_o}(t)$, for inner and outer hydrophobic regions. Careful analysis of all the individual reflectivity curves did not show any evidence or characteristic signature of an asymmetric bilayer. For any given time t the SLD values for the inner and outer tail regions were always equal (within the experimental errors). Further attempts to impose a relevant scattering difference between inner and outer hydrophobic regions failed, resulting in a model not in agreement with the experimental data. All these observations suggested that flip-flop could not be detected within the time scales probed during the NR experiments and that the time-limiting process was the lipid exchange (as further proof). The time dependence of the SLD values reported in ref 14 were used to compute the SLD values expected for the upper and lower parts of the hydrocarbon core in the presence of asymmetry and as a function of time. The time evolution of these values is shown in Figure 4 (left panel) (blue symbols). The symmetric case SLD (dark yellow curve) was extracted by assuming an undetectable flip-flop process. Reflectivity curves for asymmetric and symmetric bilayers at times $t = 1 \text{ h}$ and $t = 2.5 \text{ h}$ were computed according to the expected $\rho(t)$ values and were superimposed on the experimental data as depicted in Figure 4 (right panel). It is possible to see that, especially in the high- Q range, the asymmetric model leads to an overestimation of the reflectivity. It was verified that this was always the case,

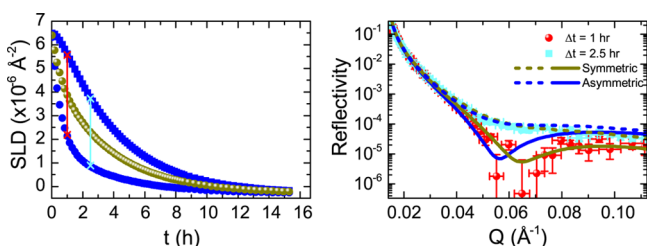


Figure 4. (Left panel) Scattering length density values for asymmetric (blue) and symmetric (dark yellow) hydrocarbon core extracted from the activation energy data published in ref 14. For the asymmetric case the outer layer (circles) is supposed to exchange material in a faster way than the inner one (squares). (Right panel) Time evolution of the reflectivity signal at 1 h (red symbols) and 2.5 h (cyan symbols) after the vesicle injection. The simulated $R(Q, t)$ curves at these given times for asymmetric and symmetric bilayer structures are plotted, respectively, as blue and dark yellow lines.

suggesting that the data do not show any asymmetry at any time. This scenario allowed us to use the symmetric model previously described.

Temperature Dependence of the Exchange Process. A typical full set of kinetics data is shown in Figure 5. The only

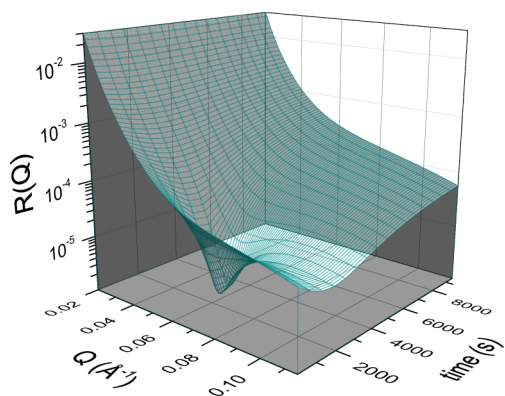


Figure 5. Time evolution of the reflectivity curves during a typical D-to-H kinetics. Data were taken from the 57 °C experiment on Figaro; the curves were smoothed for a better graphical representation.

time-dependent quantity in the analysis was SLD_{HC} modeled according to eq 2a and 2b by using the fraction of nonexchanged material $\alpha(t)$. The latter should decay from $\alpha(0) = 1$ to $\alpha(+\infty) = 0$ as shown in Figure 6. The data are shown in a semilogarithmic plot to enhance the long-term decay of the curves. The effect of temperature on the process is clearly visible. The curves decay much more rapidly as the temperature is increased. In the same graph the concentration effect is also visible. A decay curve obtained by using a vesicle concentration of 5 mg/mL is compared, at the same temperature, to the one taken with lower vesicle concentration ($c = 1$ mg/mL). Higher concentration accelerated the overall process. Both temperature and concentration effect will be discussed in the following.

The reproducibility of the measurements was ensured by comparing the results obtained using different instruments and thermodynamic conditions as shown in the Supporting Information.

The $\alpha(t)$ curves could be fitted by a single exponential decay for all the investigated samples

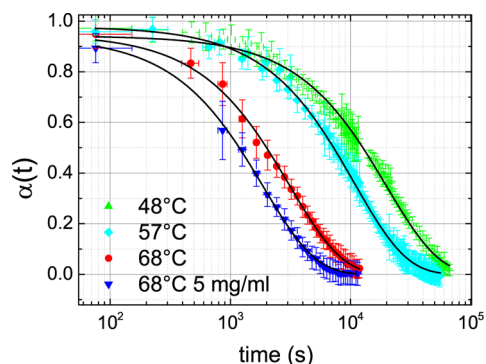


Figure 6. Content of nonexchanged molecules in the adsorbed bilayer as a function of time at different temperatures as described in the legend. Continuous lines are fits according to eq 3. Data extracted from the curves measured at 68 °C with a vesicle concentration of 5 mg/mL is plotted for comparison. Data from H-to-D and D-to-H kinetics were merged together to avoid gaps in the data as described in the text.

$$\alpha(t, T) = \alpha(0) e^{-t/\tau(T)} \quad (3)$$

where the temperature dependence is explicit. The lipid exchange resulted in a thermally activated process that followed an Arrhenius-like behavior. The activation energy of the exchange process was obtained similarly to that of reaction kinetics by

$$E_a^{ex} \equiv R \left[\frac{\partial \ln \tau(T)}{\partial (1/T)} \right] \quad (4)$$

Values for $\tau(T)$ derived according to eq 3 are plotted in Figure 7 together with a linear fit (eq 4) whose slope

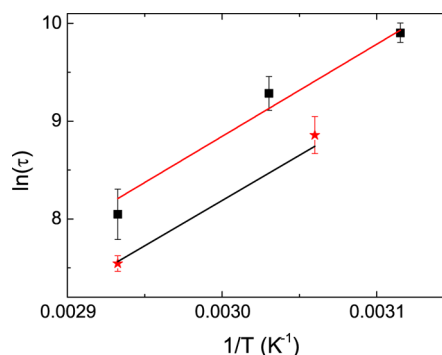


Figure 7. Arrhenius plot for the exchange kinetics measured with a vesicle concentration $c = 1$ mg/mL (squares) together with a linear fit (line) according to eq 4. $\tau(T)$ obtained with a vesicle concentration $c = 5$ mg/mL are plotted with star symbols and a parallel line to the fit is drawn as guide for the eye.

corresponds to $E_a^{ex} = 81 \pm 7$ kJ/mol. This value is in agreement with the one obtained by Nakano and co-workers (see Table 1 and ref 14) who used nonmodified DMPC molecules. The other experiments listed in Table 1 gave similar values for the activation energy but the system was not strictly the same, since they were obtained using modified or guest molecules in a DMPC matrix. The present experiment gives a clearer result regarding the exchange process, since no modification of the molecules, beside the isotopical substitution, was introduced.

Sensitivity of NR to Exchange Kinetics. During the exchange measurements, certain DMPC:d54-DMPC mixtures

may have SLD variation across the bilayer that was close to zero leading to a weak reflected signal that dropped quickly below the background threshold. The background-subtracted signal therefore had large uncertainties reflected also in the fitting parameters. This range in SLD was defined as a blind region, i.e., a region where the extracted parameters were meaningless because of the large uncertainties. The conditions for this to occur are particular to the studied system. In the present case *null* sensitivity was observed for a SLD of the hydrocarbon core (ρ_{HC} in the manuscript) ranging between 3.5 and $4.5 \times 10^{-6} \text{ \AA}^{-2}$ as shown in Figure 8. It is easy to see that the total SLD

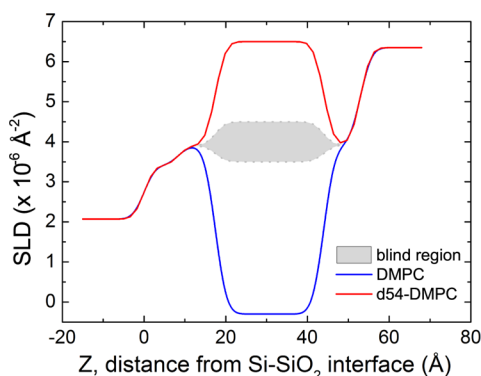


Figure 8. Scattering length density profiles for DMPC (blue) and d54-DMPC (red) in D_2O . The so-called *blind region* is highlighted by a gray area. The reflectivity signal here is affected by large uncertainties and its time-evolution could not be followed with high enough accuracy.

profile is almost flat in this range, with the SLD of the SiO_2 layer being $3.41 \times 10^{-6} \text{ \AA}^{-2}$ and that of D_2O -hydrated PC headgroups $\sim 3.9 \times 10^{-6} \text{ \AA}^{-2}$. This problem could be overcome by measuring, in the same thermodynamic conditions, the H-to-D and D-to-H kinetics. The time dependence of SLD_{HC} for the two kinetics measured at $57 \text{ }^\circ\text{C}$ is shown in Figure 9

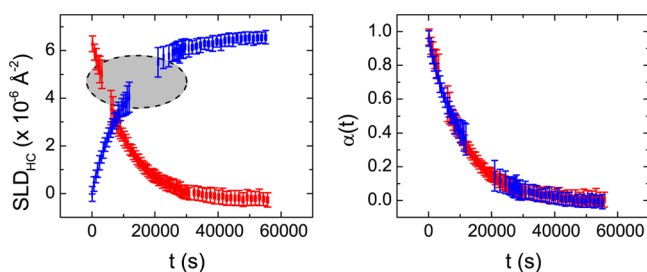


Figure 9. SLD_{HC} values (left panel) extracted from the same sample during D-to-H (red) and H-to-D (blue) kinetics. The *blind region* is indicated by the gray area. Conversion of SLD_{HC} in the content of original material $\alpha(t)$ gave two identical curves with data-gap positioned in different portion of the curves. By merging them it was possible to obtain gap-free curves as shown in the main manuscript.

(left panel). They show exactly the same time dependence, indicating no influence by the isotopic substitution. Since the SLD decay of both H-to-D and D-to-H kinetics crosses the blind region at different time ranges, we can merge the two curves to obtain a single $\alpha(t)$ decay (see Figure 9).

Kinetics measurements were performed with short acquisition times (if compared to standard measurements) and in D_2O only. Outside of the blind region changes in SLD values of

$0.1 \times 10^{-6} \text{ \AA}^{-2}$ were clearly detectable. This estimation is particular to the system investigated, and in the case of DMPC and d54-DMPC molecules, it corresponds to a 0.015 volume fraction of exchanged material.

Effect of Concentration. It is known that changes in donor/acceptor concentrations could affect the kinetics of exchange. This was shown in the case of exchange between POPC vesicles⁹ where the rate constants describing the process were concentration-dependent; the kinetics were in fact faster for a given temperature when the concentration was increased. In the present case the influence of vesicle concentration on the overall process was preliminarily investigated, showing that the kinetics were accelerated by increasing the concentration of the vesicles in the bulk (donor) up to 5 mg/mL. A typical $\alpha(t)$ curve is included in Figure 6 and the values of $\tau(T)$ measured at 68 and 54 $^\circ\text{C}$ are plotted in Figure 7 for comparison. This preliminary result showed that, for the interval of temperature considered, the activation energy was not concentration dependent because the increased concentration causes simply a global scaling of the $\tau(T)$ values.

CONCLUSIONS

While the lipid exchange process has been directly measured by several different techniques, the characteristics of lipid flip-flop to date could only be estimated for a pure DMPC system in the liquid phase, as in the case of the SANS¹⁴ experiment, or extrapolated as in the case of SFVS measurements,¹³ giving opposite results. Nakano and co-workers claimed the presence of a flip-flop process that has an activation energy of about 64 kJ/mol for pure DMPC and d54-DMPC vesicles, while Conboy and co-workers could not derive any E_a^f value because the process was too fast to be followed for a solid supported lipid bilayer in the L_α phase. The present reflectometry experiment shows that the lipid exchange features are in perfect agreement with those found by SANS, while the flip-flop appears to take place on a time-scale much faster than the experimentally accessible time-scale, set here to 2.5 min. This result is consistent with the extrapolation of SFVS data. Unfortunately, so far none of the proposed techniques were able to clarify completely the observed differences. NR and SFVS, regarding the flip-flop process, are monitoring an adsorbed bilayer where the role of defects in triggering the flip-flop process cannot be neglected.¹⁵ In the present NR experiments, defects were minimized by forming the adsorbed bilayer by vesicle fusion method. Moreover solid supported lipid bilayers were characterized by a lipid-surface interaction whose role in affecting the flip-flop kinetics, if any, is still unknown. Conversely, it is known that SANS is not able to detect directly structural asymmetry in vesicle bilayers without the choice of special contrast values.³⁹ The presence of a slow flip-flop process was introduced only in the modeling of the kinetics data to describe a nonpurely single exponential behavior. Nevertheless it is not yet clear if any other characteristic of the sample could play a role in establishing the deviation from a pure exponential law like the one observed in the NR kinetics data. As already published, the flip-flop process could be sensitive to vesicle size and therefore to sample stability and polydispersity. In conclusion, different interpretations are possible to explain the differences observed in these experiments, but an unambiguous description is still missing.

In the present work we demonstrate that neutron reflectometry is a perfect technique to investigate the processes of lipid exchange between vesicles and an adsorbed lipid bilayer,

being able to follow with a high precision the kinetics without any need of adding or using guest molecules. Moreover we report for the first time a concentration dependence of the overall exchange process. This effect, together with the influence of the surface on the overall process, will be investigated in future experiments.

■ ASSOCIATED CONTENT

● Supporting Information

The $\alpha(t,T)$ curves obtained on different instruments were highly reproducible. This material is available free of charge via the Internet at <http://pubs.acs.org/>.

■ AUTHOR INFORMATION

Corresponding Author

*E-mail: gerelli@ill.eu.

Notes

The authors declare no competing financial interest.

■ ACKNOWLEDGMENTS

We wish to thank ISIS for beamtime and ILL for beamtime and use of the PSCM facilities. We also wish to thank Richard Campbell and Maximilian Skoda for their help during the experiments and Paul Butler and Ursula Perez-Salas for useful discussions. The authors wish to thank Andrew Wildes who assisted in the proofreading of the manuscript. Y.G. acknowledges also A. de Ghellinck and E. Schneck for brainstorming and G. Allodi from Università di Parma for the development of the Fminuit minimization routine. This research project has been supported by the European Commission under the seventh Framework Programme through the "Research Infrastructures" action of the "Capacities" Programme, NMI3-II Grant number 283883.

■ REFERENCES

- (1) Devaux, P. F. Static and dynamic lipid asymmetry in cell membranes. *Biochemistry (Mosc.)* **1991**, *30*, 1163–1173.
- (2) Devaux, P. Protein involvement in transmembrane lipid asymmetry. *Annu. Rev. Biophys. Biomol. Struct.* **1992**, *21*, 417–439.
- (3) Fadeel, B.; Xue, D. The ins and outs of phospholipid asymmetry in the plasma membrane: roles in health and disease. *Crit. Rev. Biochem. Mol. Biol.* **2009**, *44*, 264–277.
- (4) Daleke, D. L. Regulation of transbilayer plasma membrane phospholipid asymmetry. *J. Lipid Res.* **2003**, *44*, 233–242.
- (5) Kornberg, R. D.; McConnell, H. M. Inside-outside transitions of phospholipids in vesicle membranes. *Biochemistry (Mosc.)* **1971**, *10*, 1111–1120.
- (6) McLaughlin, S.; Harary, H. Phospholipid flip-flop and the distribution of surface charges in excitable membranes. *Biophys. J.* **1974**, *14*, 200–208.
- (7) Sherwood, D.; Montal, M. Transmembrane lipid migration in planar asymmetric bilayer membranes. *Biophys. J.* **1975**, *15*, 417–434.
- (8) Jones, J.; Thompson, T. E. Spontaneous phosphatidylcholine transfer by collision between vesicles at high lipid concentration. *Biochemistry* **1989**, *28*, 129–134.
- (9) Jones, J. D.; Thompson, T. Mechanism of spontaneous, concentration-dependent phospholipid transfer between bilayers. *Biochemistry* **1990**, *29*, 1593–1600.
- (10) Jones, J. D.; Almeida, P.; Thompson, T. Spontaneous interbilayer transfer of hexosyl ceramides between phospholipid bilayers. *Biochemistry* **1990**, *29*, 3892–3897.
- (11) Wimley, W. C.; Thompson, T. E. Exchange and flip-flop of dimyristoyl phosphatidylcholine in liquid-crystalline, gel and two-component, two-phase large unilamellar vesicles. *Biochemistry (Mosc.)* **1990**, *29*, 1296–1303.

(12) John, K.; Schreiber, S.; Kubelt, J.; Herrmann, A.; Müller, P. Transbilayer movement of phospholipids at the main phase transition of lipid membranes: implications for rapid flip-flop in biological membranes. *Biophys. J.* **2002**, *83*, 3315–3323.

(13) Liu, J.; Conboy, J. C. 1,2-Diacyl-Phosphatidylcholine Flip-Flop Measured Directly by Sum-Frequency Vibrational Spectroscopy. *Biophys. J.* **2005**, *89*, 2522–2532.

(14) Nakano, M.; Fukuda, M.; Kudo, T.; Endo, H.; Handa, T. Determination of Interbilayer and Transbilayer Lipid Transfers by Time-Resolved Small-Angle Neutron Scattering. *Phys. Rev. Lett.* **2007**, *98*, 238101.

(15) Anglin, T.; Conboy, J. Lateral pressure dependence of the phospholipid transmembrane diffusion rate in planar-supported lipid bilayers. *Biophys. J.* **2008**, *95*, 186–193.

(16) Anglin, T.; Cooper, M.; Li, H.; Chandler, K.; Conboy, J. Free Energy and Entropy of Activation for Phospholipid Flip-Flop in Planar Supported Lipid Bilayers. *J. Phys. Chem. B* **2010**, *114*, 1903–1914.

(17) McLean, L. R.; Phillips, M. C. Kinetics of phosphatidylcholine and lysophosphatidylcholine exchange between unilamellar vesicles. *Biochemistry (Mosc.)* **1984**, *23*, 4624–4630.

(18) Jensen, E. C. Use of Fluorescent Probes: Their Effect on Cell Biology and Limitations. *The Anatomical Record: Advances in Integrative Anatomy and Evolutionary Biology* **2012**, *295*, 2031–2036.

(19) Cevc, G. *Phospholipids handbook*; Marcel Dekker, Inc., 1993.

(20) Lipowsky, R.; Sackmann, E., Eds. *Structure and Dynamics of Membranes I. From Cells to Vesicles*; Handbook of Biological Physics; Elsevier: Amsterdam, 1995; Vol. 1.

(21) Gerelli, Y.; Porcar, L.; Fragneto, G. Lipid rearrangement in DSPC:DMPC bilayers: a neutron reflectometry study. *Langmuir* **2012**, *28*, 15922–15928.

(22) Wacklin, H. P. Neutron reflection from supported lipid membranes. *Curr. Opin. Colloid Interface Sci.* **2010**, *15*, 445–454.

(23) Daillant, J.; Gibaud, A. *X-ray and neutron reflectivity: principles and applications*; Springer Verlag, 2009; Vol. 770.

(24) Garg, S.; Porcar, L.; Woodka, A.; Butler, P.; Perez-Salas, U. Noninvasive neutron scattering measurements reveal slower cholesterol transport in model lipid membranes. *Biophys. J.* **2011**, *101*, 370–377.

(25) Szoka, F., Jr; Papahadjopoulos, D. Comparative properties and methods of preparation of lipid vesicles (liposomes). *Annu. Rev. Biophys. Bioeng.* **1980**, *9*, 467–508.

(26) Campbell, R.; Wacklin, H.; Sutton, I.; Cubitt, R.; Fragneto, G. FIGARO: The new horizontal neutron reflectometer at the ILL. *Eur. Phys. J. Plus* **2011**, *126*, 1–22.

(27) Cubitt, R.; Fragneto, G. D17: the new reflectometer at the ILL. *Appl. Phys. A: Mater. Sci. Process.* **2002**, *74*, s329–s331.

(28) Webster, J.; Holt, S.; Dalglish, R. INTER the chemical interfaces reflectometer on target station 2 at ISIS. *Phys. B: Condens. Matter* **2006**, *385*, 1164–1166.

(29) Kalb, E.; Frey, S.; Tamm, L. K. Formation of supported planar bilayers by fusion of vesicles to supported phospholipid monolayers. *Biochim. Biophys. Acta - Biomembranes* **1992**, *1103*, 307–316.

(30) Wacklin, H. P. Composition and Asymmetry in Supported Membranes Formed by Vesicle Fusion. *Langmuir* **2011**, *27*, 7698–7707.

(31) Crowley, T.; Lee, E.; Simister, E.; Thomas, R. The use of contrast variation in the specular reflection of neutrons from interfaces. *Physica B* **1991**, *173*, 143–156.

(32) Knoll, W. Volume determination of deuterated dimyristoyllecithin by mass and scattering length densitometry. *Chem. Phys. Lipids* **1981**, *28*, 337–345.

(33) Nagle, J. F.; Tristram-Nagle, S. Structure of lipid bilayers. *Biochim. Biophys. Acta* **2000**, *1469*, 159–195.

(34) *MATLAB and Statistics Toolbox*, release 2012b; The MathWorks, Inc.: Natick, Massachusetts, United States.

(35) James, F. *MINUIT Function Minimization and Error Analysis*; CERN, 1998.

(36) Parratt, L. G. Surface Studies of Solids by Total Reflection of X-Rays. *Phys. Rev.* **1954**, *95*, 359–369.

(37) Richter, R.; Mukhopadhyay, A.; Brisson, A. Pathways of lipid vesicle deposition on solid surfaces: a combined QCM-D and AFM study. *Biophys. J.* **2003**, *85*, 3035–3047.

(38) Bourdieu, L.; Silberzan, P.; Chatenay, D. Langmuir-Blodgett films: From micron to angstrom. *Phys. Rev. Lett.* **1991**, *67*, 2029–2032.

(39) Sakuma, Y.; Urakami, N.; Taniguchi, T.; Imai, M. Asymmetric distribution of cone-shaped lipids in a highly curved bilayer revealed by a small angle neutron scattering technique. *J. Phys.: Condens. Matter* **2011**, *23*, 284104.